

Apralactone A and a New Stereochemical Class of Curvularins from the Marine Fungus *Curvularia* sp.

Hendrik Greve,^[a] Peter J. Schupp,^[b] Ekaterina Eguereva,^[a] Stefan Kehraus,^[a] Gerhard Kelter,^[c] Armin Maier,^[c] Heinz-Herbert Fiebig,^[c] and Gabriele M. König*^[a]

Keywords: Natural products / Marine fungi / Polyketides / Antitumor agents

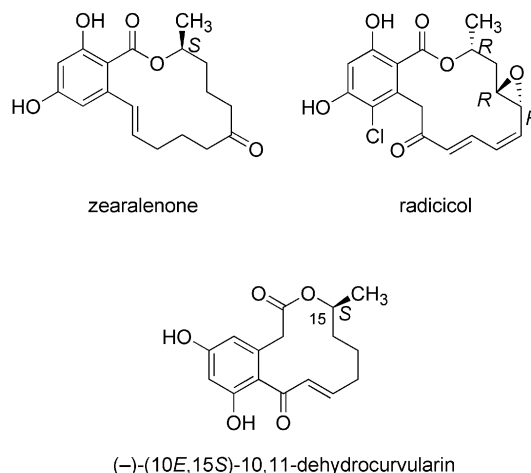
Chemical investigations of the cytotoxic extract of the marine fungus *Curvularia* sp. (strain no. 768), isolated from the red alga *Acanthophora spicifera*, yielded the novel macrolide apralactone A (**1**), as well as the antipodes of curvularin macrolides **2–7**. Compound **8**, a dimeric curvularin was recognised as an artefact. The structures of **1–8** were elucidated by interpretation of their spectroscopic data (1D and 2D NMR, CD,

MS, UV and IR). Apralactone A (**1**) is a 14-membered phenyl acetic acid macrolactone, and the first such compound with a 4-chromanone substructure. Compounds **1**, **2**, **4**, **5** and **6** were found to be cytotoxic towards human tumor cell lines with mean IC₅₀ values in the range of 1.25 to 30.06 μ M. (© Wiley-VCH Verlag GmbH & Co. KGaA, 69451 Weinheim, Germany, 2008)

Introduction

Fungal macrolides, such as zearalenone, radicicol, and the curvularin macrolides have recently attracted attention due to their interesting biological activities.^[1] Zearalenone was shown to have estrogen agonistic properties,^[2] whereas radicicol and the curvularin macrolides were found to be inhibitors of HSP90,^[3,4] a promising target for anticancer drug discovery.^[5] From the chemical point of view, the macrolides zearalenone and radicicol belong to the family of resorcylic acid lactones (RALs) possessing a C18 nonaketide backbone with a 14-membered macrolide.^[6] In contrast, the curvularins are octaketides composed of a 12-membered macrolide skeleton attached to a 3,5-dihydroxyphenylacetic acid (Scheme 1).^[7]

In continuation of our approach to isolate new bioactive secondary metabolites from marine sources, we performed chemical investigations on the cytotoxic extract of the marine fungal strain no. 768, which was identified as *Curvularia* sp.^[8] In the current study, we were able to isolate and identify the novel fungal macrolide **1**, which on the one hand is characterised by a 14-membered macrolide like in RALs (e.g., zearalenone and radicicol), but resembles the phenylacetic acid lactone moiety of the curvularins on the other hand. Such nonaketide-based carbon skeletons as for curvularins found in **1** have so far exclusively appeared in a



Scheme 1. Chemical structures of the resorcylic acid lactones zearalenone,^[1a,28a] and radicicol,^[1b,28b,28c] and the phenylacetic acid lactone (–)-(10*E*,15*S*)-10,11-dehydrocurvularin.^[7a,11]

Japanese patent as lead structure concerning the inhibition of neuro peptide Y receptor for anti-obesity programs.^[9] The structural type of **1** is unprecedented, due to the incorporation of a 4-chromanone moiety within a macrolactone. Moreover, here we describe the new stereochemical series of curvularin macrolides **2–7**.

The majority of the isolated macrolactones **1–8** were evaluated for their cytotoxic activity towards a panel of up to 36 human tumor cell lines and were found to be considerably cytotoxic in some cases. The novel macrolide **1** showed concentration-dependent cytotoxicity with a mean IC₅₀ value of 9.87 μ M. The most active metabolite, com-

[a] Institute for Pharmaceutical Biology, University of Bonn, Nussallee 6, 53115 Bonn, Germany
Fax: +49-228-733250
E-mail: g.koenig@uni-bonn.de

[b] Marine Laboratory, University of Guam, Mangilao, Guam 96923, USA

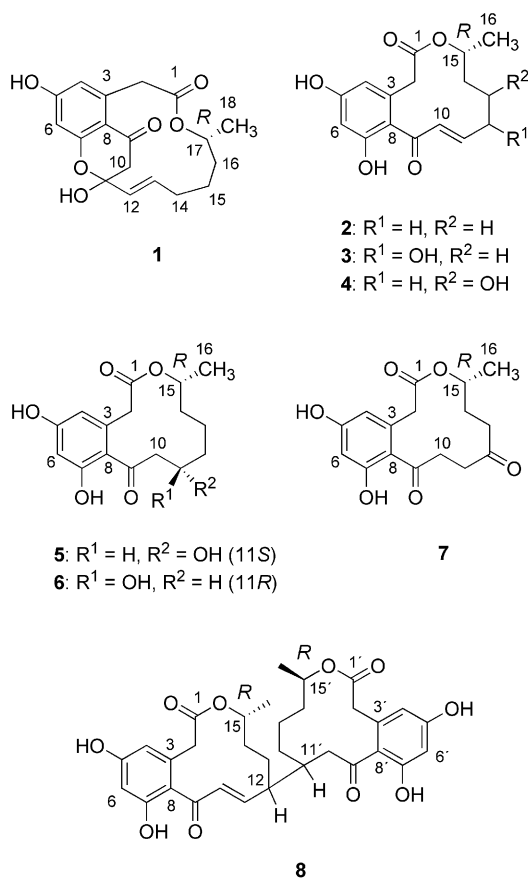
[c] Oncotest GmbH, Institute of Experimental Oncology, Am Flughafen 12–14, 79108 Freiburg, Germany

Supporting information for this article is available on the WWW under <http://www.eurjoc.org> or from the author.

pound **2**, displayed concentration-dependent cytotoxicity with a mean IC_{50} value of $1.25\ \mu\text{M}$, combined with significant in vitro tumor cell selectivity towards nine of the 36 tested tumor cell lines, which indicates 25% of selectivity.

Chemistry

The fungal strain *Curvularia* sp. (strain no. 768) was isolated from the red alga *Acanthophora spicifera* collected at Fingers Reef, Apra Harbor, Guam. Cultivation on solid biomalt medium containing artificial seawater gave a cytotoxic crude extract. Successive application of normal-phase vacuum liquid chromatography (VLC), normal- and reversed-phase HPLC yielded the novel macrolide **1**, as well as a new stereochemical class of curvularins **2–7**, and the dimeric artefact **8** (Scheme 2).



Scheme 2. Secondary metabolites **1–7**, isolated from *Curvularia* sp., and artefact **8**.

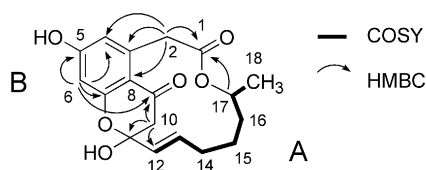
The empirical formula of **1** was determined as $\text{C}_{18}\text{H}_{20}\text{O}_6$ by high resolution ESI-MS implying nine elements of unsaturation (m/z 331.1187 [$\text{M} - \text{H}$] $^-$, Δ +0.5 mmu). Inspection of the ^1H and ^{13}C NMR spectra (Table 1) in combination with the DEPT and ^1H – ^{13}C HSQC data of **1** revealed the presence of two *meta*-positioned aromatic protons (4-H, $\delta_{\text{H}} = 6.34$ ppm, d, 2.2 Hz and 6-H, $\delta_{\text{H}} = 6.38$ ppm, d, 2.2 Hz), two olefinic *trans*-oriented protons (12-H, $\delta_{\text{H}} =$

5.34 ppm, d, 15.7 Hz and 13-H, $\delta_{\text{H}} = 5.58$ ppm, dt, 15.7, 7.5 Hz), an oxygen-substituted methine group (17-CH, $\delta_{\text{C}} = 69.3$ ppm; $\delta_{\text{H}} = 5.03$ ppm), two isolated methylene groups whose protons exclusively display geminal coupling ($^2J_{2a/2b} = 16.5$ Hz; $^2J_{10a/10b} = 16.0$ Hz), three further methylene groups (14-CH₂, 15-CH₂, and 16-CH₂), and one methyl group (18-CH₃, $\delta_{\text{C}} = 17.5$ ppm; $\delta_{\text{H}} = 0.96$ ppm). Moreover, resonance signals for six sp^2 quaternary carbons were detected, whereof one is attributable to a ketone carbonyl (C-9, $\delta_{\text{C}} = 192.1$ ppm) and one to an ester carbonyl group (C-1, $\delta_{\text{C}} = 169.4$ ppm). The chemical shift of the remaining ^{13}C resonance signal at $\delta = 102.2$ ppm (C-11, C_{quat}) suggested to arise from a sp^3 -hybridised carbon atom, which bears two oxygen functionalities.

^1H – ^1H COSY and ^1H – ^{13}C HMBC NMR experiments allowed us to deduce the gross structure of **1** as shown in Figure 1. The spin system beginning with 12-H and continuing through to 18-H₃ could be concluded on the basis of the ^1H – ^1H COSY correlations (fragment A, Figure 1). The geometry of the Δ^{12} double bond was assigned as 12*E* from the ^1H – ^1H coupling constant ($^3J_{12/13} = 15.7$ Hz). The second part of the molecule (C-1 to C-11) included seven quaternary carbon atoms and had to be established using HMBC correlations (fragment B, Figure 1). The phenylacetic acid substructure was inferred from diagnostic cross-peaks between the resonances for 2-Ha/2-Hb and C-1, C-3, C-4 and C-8, and between 6-H and C-4, C-5, C-7 and C-8 (Table 1). The deshielded ^{13}C NMR resonances for C-5 and C-7 ($\delta_{\text{C}} = 163.7$ and 164.3 ppm, respectively) indicated a substitution with oxygen. Coupling between 6-H and C-9, as well as between 10-Ha/10-Hb and both C-9 and C-11 gave evidence for the benzylic ketone nature of **1**. Fragments A and B were found to be connected between C-1 and the oxygen-bearing methine group 17-CH via an ester bond and between the quaternary carbon C-11 and the olefinic methine group 12-CH due to the HMBC correlations from 17-H to C-1 and from 10-Ha/10-Hb to C-12, respectively. At this stage of the structural analysis, the remaining element of unsaturation had to be taken care of and a ring closure via a hemiketal linkage between the oxygen-functionalised carbon atoms C-7 and C-11 to form a common 4-chromanone ring system was most likely. This assumption was strongly supported by the ^{13}C NMR chemical shifts of C-3 to C-11 and the ^1H NMR resonances attributable to the two exchangeable hydroxyl protons 5-OH and 11-OH ($\delta_{\text{H}} = 6.52$ and 9.41 ppm, respectively; Table 1), which are highly consistent with the respective values of a 4-chromanone moiety with an identical substitution pattern to that of **1** reported for the polyketides SEK4 and SEK4b.^[10] Finally, the planar structure of **1** matches the molecular formula requirements including its nine elements of unsaturation and the trivial name apralactone A is suggested for **1**. The absolute configuration of **1** at the chiral center C-17 was subsequently concluded as (17*R*) by comparison of its CD spectrum with the CD spectra of the structurally related curvularins **2–7**, in particular regarding the comparable Cotton effect of **1** with a maximum at 215 nm.

Table 1. NMR spectroscopic data for **1** in [D₆]acetone (δ in ppm, mult., *J* in Hz).

No.	δ C	δ H	¹ H- ¹ H COSY	HMBC
1	169.4, C _{quat}			
2	42.8, CH ₂	a: 3.41 (d, 16.5) b: 4.13 (d, 16.5)	2b 2a	1, 3, 4, 7 ^[a] , 8 1, 3, 4, 7 ^[a]
3	140.3, C _{quat}			
4	114.3, CH	6.34 (d, 2.2)	6	1, 2, 5, 6, 8, 9
5	163.7, C _{quat}			
6	102.7, CH	6.38 (d, 2.2)	4	4, 5, 7, 8, 9
7	164.3, C _{quat}			
8	113.7, C _{quat}			
9	192.1, C _{quat}			
10	49.5, CH ₂	a: 2.76 (d, 16.0) b: 3.03 (d, 16.0)	10b 10a	3 ^[a] , 7 ^[a] , 8, 9, 11, 12 9, 11, 12, 13 ^[a]
11	102.2, C _{quat}			
12	129.3, CH	5.34 (d, 15.7)	13	10, 11, 13, 14, 15 ^[a]
13	134.9, CH	5.58 (dt, 15.7, 7.5)	12, 14a, 14b	11, 12, 14, 15 ^[a]
14	30.9, CH ₂	a: 1.57 (m) b: 2.04 (m)	13, 14b, 15a 13, 14a, 15a, 15b	12, 13, 15, 16 12, 13, 15 ^[a] , 16 ^[a]
15	22.3, CH ₂	a: 0.68 (q, 11.7) b: 1.52 (m)	14a, 14b, 15b, 16 14b, 15a, 16	13 ^[a] , 16, 17 ^[a] 13 ^[a] , 16
16	31.5, CH ₂	1.29 (m)	15a, 15b, 17	14, 15, 18
17	69.3, CH	5.03 (m)	16, 18	1, 15, 16, 18
18	17.5, CH ₃	0.96 (d, 6.6)	17	16, 17
OH		9.41, s, 1 H ^[b]		
OH		6.52, br. s, 1 H ^[b]		

[a] Weak signal. [b] Signals detected in [D₈]THF.Figure 1. ¹H-¹H COSY and selected ¹H-¹³C long-range correlations of **1**.

The NMR spectroscopic data of **2**, **3**, and **5–7** are in full agreement with the previously published values for their enantiomers (Tables S1 and S2, Supporting Information).^[7b,11–13] All planar structures of **2–7** were confirmed by interpretation of extensive 1D and 2D NMR experiments (HMBC, HSQC, COSY). The absolute configuration (15*S*) of the published curvularins was determined via total synthesis of (–)-(15*S*)-curvularin and by degradation of (–)-(10*E*,15*S*)-10,11-dehydrocurvularin.^[7a,14] On the basis of their optical rotation and CD spectra, the newly isolated curvularin-type metabolites **2–7** were found to possess a different configuration at C-15, which was assigned as (15*R*) when compared to the known compounds.^[7b,11–13] As it is shown in Table 2, the optical rotation of compounds **2**, **3**, and **5–7** corresponds regarding its magnitude to values in the literature, but has the opposite sign. Moreover, the Cotton effect observed in the CD spectra attributable to the $n-\pi^*$ transition band of the lactone at around 229–235 nm of compounds **2–7** showed the opposite sign to that reported for (–)-(10*E*,15*S*)-10,11-dehydrocurvularin (Table 2).^[15] Thus, compound **2** proved to be (+)-(10*E*,15*R*)-10,11-dehydrocurvularin (Scheme 2).^[11]

Compound **3** is the 12-hydroxy derivative of **2**. A compound with this basic structure and 15*S* configuration has been reported, however stereochemical assignment at the hydroxylated carbon C-12 was not done. Our data show that metabolite **3** is the antipode of the reported compound.^[12]

Mass and NMR spectral analysis revealed compound **4** to be a new positional isomer of **3**. In the case of **4**, no enantiomer is described in the literature. Instead of the 12-hydroxy group in **3**, compound **4** exhibits a hydroxyl group at position C-13, as evident from the spin system beginning with 10-H through to 16-H₃, which was deduced from the ¹H-¹H COSY correlations. The deshielded ¹³C NMR resonances for C-13 ($\delta_c = 66.9$) clearly supported the substitution of this carbon with a hydroxyl functionality.

Compounds **5** and **6** are epimers concerning the hydroxyl-bearing stereocenter C-11. Compound **5** is the enantiomer of the known (–)-(11*R*,15*S*)-11-hydroxycurvularin, while **6** is the enantiomer of the reported (–)-(11*S*,15*S*)-11-hydroxycurvularin.^[13] The absolute configurations of **5** and **6** were assigned as (11*S*,15*R*) and (11*R*,15*R*), respectively, by comparing the optical rotation and ¹H NMR spectroscopic data with those of the reported enantiomeric counterparts.^[12,13] Compounds **5** and **6** are thus (+)-(11*S*,15*R*)-11-hydroxycurvularin and (+)-(11*R*,15*R*)-11-hydroxycurvularin, respectively. Compound **7** proved to be (+)-(15*R*)-12-oxocurvularin, based on the comparison of the optical rotation and ¹H and ¹³C NMR spectroscopic data with those of the reported enantiomeric counterpart.^[12,13]

Accurate mass measurement of compound **8** (HREIMS, *m/z* 580.2309 [M]⁺) indicated it to have twice the mass of compound **2** and therefore the elemental composition

Table 2. Chiroptical data of compounds **1–7** in comparison with the published values of the corresponding enantiomers given in the literature.

	Measured $[\alpha]_D$ (EtOH)	$[\alpha]_D$ (EtOH) of the enantiomer	Measured Cotton effect in the CD spectrum (216–235 nm, MeOH)	Cotton effect of the enantiomer (MeOH)
1	$[\alpha]_D^{22} = +10.0$ ($c = 0.3$)	n.e. ^[b]	$\Delta\epsilon = 216$ (+8.22)	n.e. ^[b]
2	$[\alpha]_D^{22} = +79.1$ ($c = 0.4$)	$[\alpha]_D^{22} = -79.8$ ($c = 3.0$) ^[11a]	$\Delta\epsilon = 229$ (+6.84)	$\Delta\epsilon = 235$ (−4.79) ^[15]
3	$[\alpha]_D^{25} = +49.9$ ($c = 0.09$)	$[\alpha]_D^{26} = -49.5$ ($c = 0.86$) ^[12]	$\Delta\epsilon = 230$ (+4.12)	n.d. ^[a]
4	$[\alpha]_D^{25} = +126.5$ ($c = 0.29$)	n.e. ^[b]	$\Delta\epsilon = 231$ (+5.49)	n.e. ^[b]
5	$[\alpha]_D^{22} = +6.9$ ($c = 0.47$)	$[\alpha]_D^{24} = -10.9$ ($c = 0.19$) ^[13]	$\Delta\epsilon = 229$ (+5.06)	n.d. ^[a]
6	$[\alpha]_D^{22} = +25.2$ ($c = 0.26$)	$[\alpha]_D^{26} = -29.4$ ($c = 0.33$) ^[13]	$\Delta\epsilon = 229$ (+1.20)	n.d. ^[a]
7	$[\alpha]_D^{22} = +53.8$ ($c = 0.13$)	$[\alpha]_D^{29} = -43.5$ ($c = 0.47$) ^[13]	$\Delta\epsilon = 230$ (+3.73)	n.d. ^[a]

[a] n.d.: not determined in the literature. [b] n.e.: no enantiomer reported in the literature.

Table 3. NMR spectroscopic data for **8** in $[D_6]$ acetone (δ in ppm, mult., J in Hz).

(10 <i>E</i>)-10,11-Dehydrocurvularin part of 8			Curvularin part of 8		
No.	δ C	δ H	No.	δ C	δ H
1	171.5, C _{quat}		1'	170.5, C _{quat}	
2	42.9, CH ₂	a: 3.67 (d, 17.9) b: 4.04 (d, 17.9)	2'	40.7, CH ₂	a: 3.63 (d, 15.8) b: 3.96 (d, 15.8)
3	138.3, C _{quat}		3'	138.4, C _{quat}	
4	113.1, CH	6.33 ^[a]	4'	112.7, CH	6.33 ^[a]
5	162.4, C _{quat}		5'	160.6, C _{quat}	
6	102.8, CH	6.32 ^[a]	6'	102.7, CH	6.41 (d, 2.2)
7	165.0, C _{quat}		7'	159.3, C _{quat}	
8	116.6, C _{quat}		8'	119.9, C _{quat}	
9	196.7, C _{quat}		9'	205.0, C _{quat}	
10	131.1, CH	6.67 (d, 15.7)	10'	47.4, CH ₂	a: 2.66 (dd, 10.0, 15.0) b: 2.99 (d, 15.0)
11	152.7, CH	6.83 (dd, 7.7, 15.7)	11'	39.8, CH	2.16 (m)
12	44.5, CH	2.42 (q, 7.7)	12'	30.9, CH ₂	a: 1.30 ^[a] b: 1.43 ^[a]
13	26.7, CH ₂	a: 1.53 (m) b: 2.00 (m)	13'	20.1, CH ₂	1.33 ^[a]
14	33.7, CH ₂	a: 1.63 ^[a] b: 1.74 (m)	14'	32.4, CH ₂	a: 1.34 ^[a] b: 1.64 ^[a]
15	72.0, CH	4.64 (m)	15'	71.0, CH	4.99 (m)
16	19.9, CH ₃	1.18 (d, 6.6)	16'	19.1, CH ₃	1.06 (d, 6.6)
OH					9.24 (br. s, 3 H), 12.12 (br. s, 1 H)

[a] Overlapped resonance signals.

C₃₂H₃₆O₁₀, implying fifteen elements of unsaturation. These data suggested **8** to be a dimeric curvularin. Its ¹H and ¹³C NMR spectra displayed resonance signals attributable to a (10*E*)-10,11-dehydrocurvularin and a curvularin part in the ratio 1:1 (Table 3). Structure elucidation of **8** was based on extensive 1D and 2D NMR experiments (HMBC, HSQC, COSY). The connection between the (10*E*)-10,11-dehydrocurvularin and the curvularin part was established between C-12 and C-11' due to an observed ¹H–¹H COSY correlation from 12-H ($\delta_H = 2.42$ ppm) to 11'-H ($\delta_H = 2.16$ ppm), and moreover HMBC correlations from both 10-H ($\delta_H = 6.67$ ppm) and 11-H ($\delta_H = 6.83$ ppm) to C-11' ($\delta_C = 39.8$ ppm), and from 10'-Hb ($\delta_H = 2.99$ ppm) to C-12 ($\delta_C = 44.5$ ppm) (see Figures S9-1 and S9-2 in the Supporting Information). Selective NOE measurements confirmed the gross structure of **8**, since irradiation at the resonance frequency of 11'-H ($\delta_H = 2.16$ ppm) caused enhancement of the resonance for 12-H ($\delta_H = 2.42$ ppm) (Figure S9-3, Supporting Information). Thus, **8** was identified as

the first curvularin-type dimer. HPLC-ESI-MS experiments, however gave evidence for **8** being an artefact. It was shown that **8** is a dimerisation product of **2** formed during the extraction procedure. We consider a Michael addition with compound **2** reacting on the one hand as Michael donor and on the other hand as Michael acceptor, which is consistent with the *trans*-olefinic 1,7-diketone moiety of **8** as reaction product. The absolute configuration of **8** is hence assumed as (15*R*,15'*R*) but remains unresolved at the stereogenic centers C-12 and C-11'.

Biological Results

The cytotoxicity of macrolides **1**, **2**, **4**, **5**, **6**, and **8** was determined in a monolayer cell survival and proliferation assay. For the assays a panel of up to 36 human tumor cell lines, comprising 14 different solid tumor types was used. The examined macrolides showed different activities, ex-

Table 4. Cytotoxic activities of **1**, **2**, **4**, **5**, **6**, and **8**.

Tumor type	Cell line	IC ₅₀ [μM]					
		1	2	4	5	6	8
Bladder	BXF 1218L	12.3	0.43	12.3	7.34	13.17	>17.22
	BXF T24	6.36	0.5	>32.64	3.14	10.67	>17.22
Glioblastoma	CNXF 498NL	n.d. ^[a]	1.98	13.88	1.75	11.34	>17.22
	CNXF SF268	6.85	0.36	24.01	2.96	10.12	>17.22
Colon	CXF HCT116	9.59	3.35	>32.64	11.11	21.2	>17.22
	CXF HT29	10.26	3.22	>32.64	8.78	13.0	>17.22
Stomach	GXF 251L	9.35	0.81	>32.64	12.51	16.66	>17.22
Head & neck	HNXF 536L	n.d.	1.84	15.55	7.35	8.0	>17.22
Lung	LXF 1121L	11.43	1.56	23.67	7.66	13.63	>17.22
	LXF 289L	15.77	0.28	>32.64	13.34	17.92	>17.22
	LXF 526L	4.61	1.11	>32.64	9.63	16.18	>17.22
	LXF 529L	n.d.	1.4	>32.64	3.59	9.78	>17.22
	LXF 629L	9.71	2.17	>32.64	7.93	13.31	>17.22
	LXF H460	6.74	2.88	>32.64	11.2	17.11	>17.22
	MAXF 401NL	9.17	0.4	16.99	1.86	16.87	>17.22
Breast	MAXF MCF7	10.11	2.63	>32.64	4.44	11.31	>17.22
	MEXF 276L	9.03	5.45	21.47	14.04	19.01	>17.22
Melanoma	MEXF 394NL	n.d.	0.68	14.31	0.92	2.05	>17.22
	MEXF 462NL	12.2	0.38	>32.64	10.96	13.45	>17.22
	MEXF 514L	n.d.	0.5	>32.64	3.84	14.77	>17.22
	MEXF 520L	7.66	1.27	25.93	2.22	10.26	>17.22
	OVXF 1619L	n.d.	1.75	>32.64	6.04	8.02	>17.22
Ovary	OVXF 899L	9.56	0.58	>32.64	10.61	11.23	>17.22
	OVXF OVCAR3	10.97	1.84	>32.64	13.09	23.46	>17.22
	PAXF 1657L	13.25	4.54	32.64	14.14	18.0	>17.22
Pancreas	PAXF PANC1	11.43	1.99	>32.64	4.02	10.77	>17.22
	PRXF 22RV1	7.66	0.76	>32.64	2.5	11.45	>17.22
Prostate	PRXF DU145	7.94	0.81	>32.64	2.44	9.77	>17.22
	PRXF LNCAP	9.52	3.75	>32.64	6.55	20.46	>17.22
	PRXF PC3M	10.05	0.4	>32.64	3.24	9.58	>17.22
Mesothelioma	PXF 1752L	16.78	0.79	28.18	16.21	>32.43	>17.22
Kidney	RXF 1781L	16.57	2.14	>32.64	12.04	15.73	>17.22
	RXF 393NL	n.d.	2.03	>32.64	11.9	15.5	>17.22
	RXF 486L	12.64	3.27	>32.64	9.07	14.88	>17.22
	RXF 944L	n.d.	2.31	33.94	4.57	11.84	>17.22
Uterus	UXF 1138L	10.11	0.89	>32.64	8.96	12.48	>17.22
Mean		9.87	1.25	30.06	6.09	12.99	>17.22

[a] n.d.: not determined.

pressed by mean IC₅₀ values ranging from 1.25 μM to 30.06 μM (Table 4). Compound **8** did not show cytotoxic activity in the test range up to 17.2 μM. The novel macrolide apralactone **A** (**1**) showed moderate concentration-dependent cytotoxicity with a mean IC₅₀ value of 9.87 μM. The most active metabolite, compound **2**, displayed concentration-dependent cytotoxicity with a mean IC₅₀ value of 1.25 μM, combined with significant in vitro tumor cell selectivity towards nine of the 36 tested tumor cell lines, which indicates 25% of selectivity (using an individual IC₅₀ value < 1/2 of the mean IC₅₀ value as threshold for above average sensitivity). These nine above average sensitive cell lines were BXF 1218L (bladder cancer, IC₅₀ = 0.43 μM), BXF T24 (bladder cancer, IC₅₀ = 0.5 μM), CNXF SF268 (glioblastoma, IC₅₀ = 0.36 μM), LXF 289L (lung adenocarcinoma, IC₅₀ = 0.28 μM), MAXF 401NL (mammary cancer, IC₅₀ = 0.4 μM), MEXF 462NL (melanoma, IC₅₀ = 0.38 μM), MEXF 514L (melanoma, IC₅₀ = 0.5 μM), OVXF 899L (ovarian cancer, IC₅₀ = 0.58 μM), and PRXF PC3M (prostate cancer, IC₅₀ = 0.4 μM) (Table 4).

Discussion

Fungal phenylacetic acid lactones (PALs) were to date reported either with a 10-membered macrolactone like xes-todecalactones **A** and **B**, and sporostatin (C14 carbon skeleton),^[16] or a 12-membered lactone ring as in the curvularins (C16 carbon skeleton).^[11–13] PALs with a 14-membered ring like in **1** (C18 carbon skeleton) have to date only been reported in the patent literature.^[9] 14-Membered macrolides from fungal sources are, however, quite common in the class of the resorcylic acid lactones (RALs) like zearalenone and radicicol,^[1a–1c] and only a few RALs have been described, which possess a 12-membered macrolactone (e.g. lasiodiplodin, *cis*- and *trans*-resorcylicides).^[17] Both, PALs and RALs have been isolated from many fungal taxa; PALs were obtained from e.g., *Curvularia*,^[1d,11a] *Memnoniella*,^[9] *Penicillium*,^[11b–13,16a,18] *Sporormiella*,^[16b] *Alternaria*,^[19] *Aspergillus*,^[20] and *Stemphylium*,^[21] and RALs e.g., from *Gibberella*,^[1a] *Nectria*,^[1b] *Lasiodiplodia*^[17a] and *Penicillium*.^[17b,17c]

From the biosynthetic point of view, both, the RALs and PALs were illustrated to be polyketides.^[6,7] Both macrolide classes apparently have varied oxidation levels around the macrocycles. Even though 4-chromanone moieties are rather common in nature, their incorporation in a macrolactone ring as found in **1** is to our best knowledge unique among macrolides. 4-chromanone ring systems are characteristic for flavonoids, in particular flavanones,^[22] but they also occur typically as parts of fungal naphtho- γ -pyrones (e.g., nigerasperones B–C, fonsecinones B–D, aurosperson B, and fonsecin),^[23] and fungal xanthenes (e.g., monodictysins A–C, monodictyxanthone, and ascherxanthone A).^[24] Furthermore, 4-chromanone substructures have been also reported to appear in rather rare secondary metabolites of fungal origin, such as the brocaenols A–C, lachnones C–E, cavoxone, and polivione.^[25] The formation of the hemiketal linkage of the 4-chromanone moiety was proposed to occur in a non-catalytic way during the polyketide biosynthesis of SEK4 and SEK4b in *Streptomyces* as a result of an intramolecular attack of a hydroxyl onto a ketone.^[10] Hemiketals are quite usual among natural products and were found in the above discussed fungal naphtho- γ -pyrones as functional group of the 4-chromanone element, but have also been described in more prominent structures like the polyketidic polyene antifungals amphotericin B and nystatin A₁,^[26] as well as in members of the marine antitumor compounds dolastatins and bryostatins.^[27]

The configuration at the lactone bearing stereogenic center is obviously variable among the PALs and RALs. The latter include for example, zearalenone and radicicol with the absolute *S* and *R* configuration, respectively, at the lactone bearing chiral center.^[28] The former include, on the one hand, the (–)-(15*S*)-curvularin macrolides, and on the other hand our newly identified (+)-(15*R*)-curvularin series (**2–7**), (+)-(17*R*)-apralactone A (**1**), as well as the described macrolide xestodecalactone A, exhibiting the absolute *R* configuration at the comparable stereogenic center.^[29] Thus, it has to be concluded that the reduction of the β -keto group via β -ketoacyl reductases creates variable configurations within fungal macrolide biosynthesis.^[7a]

Members of the phenylacetic acid lactones have been evaluated for their anticancer potential. The 10-membered PAL sporostatin was illustrated to inhibit the epidermal growth factor (EGF) receptor tyrosine kinase in vitro, which is discussed as target for anticancer therapy,^[16b] and the 10-membered PAL xestodecalactone has been patented for its antitumor activity.^[30] (–)-(15*S*)-curvularin-type metabolites were reported to be cytotoxic against human cancer cell lines,^[11b] and their mode of action as HSP90 inhibitors has been patented.^[4] In the current study, the newly identified (+)-(15*R*)-curvularin-type metabolites **2**, **4**, **5** and **6** were found to exhibit structure-dependent cytotoxic properties. Especially, (+)-(10*E*,15*R*)-10,11-dehydrocurvularin (**2**) displayed strong cytotoxicity against human cancer cell lines in a concentration-dependent manner (mean IC₅₀ = 1.25 μ M), indicating that the stereochemistry at the chiral center C-15 of the curvularin macrolides is not crucial for their cytotoxic activity. In contrast, variations of the ox-

idation levels around the macrocycle seem to influence the cytotoxic activity of the (+)-(15*R*)-curvularin-type metabolites, as shown impressively in the case of compound **4** (mean IC₅₀ = 30.06 μ M). Compound **2** possesses about 24-fold more cytotoxic potency than its 13-hydroxy derivative **4** concerning their mean IC₅₀ values. Other structural variations of **2**, like the extended and modified macrocycle found in **1** (mean IC₅₀ = 9.87 μ M) and the dimeric structure of **8** (mean IC₅₀ > 17.22 μ M) also decrease cytotoxic activity.

Experimental Section

General: Optical rotation was measured on a JASCO DIP 140 polarimeter. UV and IR spectra were obtained employing Perkin–Elmer Lambda 40 and Perkin–Elmer Spectrum BX instruments, respectively. CD spectra were recorded in MeOH and CH₃CN at room temperature with a JASCO J-810–150S spectropolarimeter; the path length was $d = 0.1$ cm. ¹H, ¹³C, COSY, NOESY, HSQC, and HMBC NMR spectra were recorded in [D₆]acetone or [D₈]THF using a Bruker Avance 300 DPX spectrometer operating at 300 MHz for proton and at 75 MHz for ¹³C. Selective one-dimensional NOE NMR spectroscopy was achieved in [D₆]acetone as solvent utilizing a Bruker Avance 500 DRX spectrometer operating at 500 MHz. Spectra were referenced to the residual solvent signal of [D₆]acetone or [D₈]THF with resonances at $\delta_{H/C} = 2.04/29.8$ and $\delta_H = 1.72$, respectively. LRESIMS measurements were performed employing an API 2000, Triple Quadrupole LC/MS/MS, Applied Biosystems/MDS Sciex and ESI source. HREIMS was recorded on a Finnigan MAT 95 spectrometer, and HRESIMS on a Bruker Daltonik micrOTOF-Q Time-of-Flight mass spectrometer with ESI source. Preparative HPLC was carried out using a Waters 515 HPLC pump and a Knauer K-2300 differential refractometer as detector.

Isolation and Taxonomy of the Fungal Strain: The red alga *Acanthophora spicifera* was collected in 2–4 m depth by snorkelling at Fingers Reef, Apra Harbor, Guam. After surface sterilization of the algae with 70% ethanol, algal samples were rinsed with sterile water and pressed onto biomalt agar plates to detect the presence of any fungal spores on the surface of alga. Sterilized alga was then cut into pieces and placed on agar plates containing isolation medium: 15 g/L agar, artificial seawater, benzyl penicillin (250 mg/L), and streptomycin sulfate (250 mg/L). Fungal colonies growing out of the algal tissue were transferred to medium for sporulation (15 g/L agar, 20 g/L biomalt extract, artificial seawater). The fungal strain was identified as *Curvularia* sp. by the Centraalbureau voor Schimmelcultures, Utrecht, The Netherlands.

Cultivation: The fungal strain (strain number 768, culture collection of Institute for Pharmaceutical Biology, University of Bonn, Germany) was cultivated at room temperature for seven weeks in 38 Fernbach flasks (250 mL each). The solid biomalt medium contained 20 g/L of Biomalt (Villa Natura Gesundheitsprodukte GmbH, Germany), 15 g/L agar (Fluka Chemie AG), and artificial seawater [(g/L): KBr (0.1), NaCl (23.48), MgCl₂·6H₂O (10.61), CaCl₂·2H₂O (1.47), KCl (0.66), SrCl₂·6H₂O (0.04), Na₂SO₄ (3.92), NaHCO₃ (0.19), H₃BO₃ (0.03)].

Extraction and Isolation: Cultivation medium (9.5 L) and mycelia were extracted with ethyl acetate (3 \times 5 L) after being homogenized using an Ultra Turrax. The ethyl acetate crude extract (3.55 g, reddish, oily) was fractionated via normal-phase VLC (13 \times 4 cm, silica gel 60, 0.063–0.200 mm, Merck, Darmstadt, Germany) with a CH₂Cl₂/EtOAc/MeOH gradient in 10 steps to yield 10 fractions.

Fractions 3 and 4 were of further interest because of their cytotoxic activity and ^1H NMR spectra. Fraction 3 was separated again by normal-phase VLC (13 \times 4 cm, silica gel 60, 0.063–0.200 mm, Merck, Darmstadt, Germany), this time using a petroleum ether/EtOAc/MeOH gradient to yield 11 subfractions, whereof subfraction 8 was purified via RP-HPLC (column: Macherey–Nagel, Nucleodur 100, C18-ec, 5 μm , 250 \times 8 mm; MeOH/H₂O, 60:40; 2 mL/min) to afford pure compound **2** (38.6 mg). Fraction 4 was separated by normal-phase HPLC (column: Knauer, Eurospher-100-Si, 5 μm , 250 \times 8 mm; petroleum ether/acetone, 80:20; 2 mL/min) to obtain pure compounds **3** (1.3 mg), **4** (4.3 mg), and **8** (13.9 mg), impure compounds **1** and **7**, and a mixture of **5** and **6**. Required purification of **1**, **7**, and the mixture of **5** and **6** was achieved via RP-HPLC (column: Macherey–Nagel, Nucleodur 100, C18-ec, 5 μm , 250 \times 8 mm; 2 mL/min) applying MeOH/H₂O, 50:50, to yield pure compound **1** (5.0 mg), and using MeOH/H₂O, 35:65, to give pure compounds **7** (1.2 mg), **5** (7.0 mg) and **6** (3.9 mg), respectively.

Apralactone A (1): Colourless amorphous solid (5.0 mg, 0.1%), $[\alpha]_{\text{D}}^{22} = +10.0$ ($c = 0.3$, EtOH). UV (EtOH): λ_{max} (ϵ) = 216 (14720), 239 (9813), 280 (10981), 312 nm (5607). CD ($c = 1.1 \times 10^{-3}$ mol/L, MeOH): λ_{max} ($\Delta\epsilon$) = 203 (+12.69), 216 (+8.22), 277 (+4.82), 309 (−6.65), 332 nm (+3.08). CD ($c = 1.1 \times 10^{-3}$ mol/L, CH₃CN): λ_{max} ($\Delta\epsilon$) = 203 (+12.97), 215 (+11.47), 275 (+6.40), 308 (−7.35), 331 nm (+3.31). IR (ATR): $\tilde{\nu}_{\text{max}}$ = 3284 (br), 2927, 1698, 1607, 1584, and 1278 cm^{-1} . ^1H and ^{13}C NMR spectroscopic data (Table 1); LRESIMS m/z 331 $[\text{M} - \text{H}]^-$. HRESIMS calcd. for C₁₈H₁₉O₆ $[\text{M} - \text{H}]^-$ m/z 331.1182, found m/z 331.1187.

(+)-(10E,15R)-10,11-Dehydrocurvularin (2): Colourless amorphous solid (38.6 mg, 1.1%), $[\alpha]_{\text{D}}^{22} = +79.1$ ($c = 0.4$, EtOH). UV (EtOH): λ_{max} (ϵ) = 224 (12403), 298 (5233), 337 nm (4457). CD ($c = 1.7 \times 10^{-3}$ mol/L, MeOH): λ_{max} ($\Delta\epsilon$) = 229 nm (+6.84). IR (ATR): $\tilde{\nu}_{\text{max}}$ = 3333 (br), 2932, 1727, 1704, 1620, 1592, 1194, and 1173 cm^{-1} . ^1H and ^{13}C NMR spectroscopic data (Tables S1 and S2, Supporting Information); LRESIMS: m/z = 291 $[\text{M} + \text{H}]^+$. HRESIMS calcd. for C₁₆H₁₉O₅ $[\text{M} + \text{H}]^+$ m/z 291.1232, found m/z 291.1227.

(+)-(10E,15R)-12-Hydroxy-10,11-dehydrocurvularin (3): Colourless amorphous solid (1.3 mg, 0.04%), $[\alpha]_{\text{D}}^{25} = +49.9$ ($c = 0.09$, EtOH). UV (EtOH): λ_{max} (ϵ) = 225 (22511), 284 (7044), 312 (6126), 333 nm (4747). CD ($c = 1.6 \times 10^{-3}$ mol/L, MeOH): λ_{max} ($\Delta\epsilon$) = 230 (+4.12), 309 (−0.74), 338 nm (+0.48). IR (ATR): $\tilde{\nu}_{\text{max}}$ = 3285 (br), 2926, 1698, 1614, 1591, 1264 and 1162 cm^{-1} . ^1H and ^{13}C NMR spectroscopic data (Tables S1 and S2, Supporting Information); LRESIMS: m/z = 307 $[\text{M} + \text{H}]^+$. HRESIMS calcd. for C₁₆H₁₉O₆ $[\text{M} + \text{H}]^+$ m/z 307.1182, found m/z 307.1176.

(+)-(10E,15R)-13-Hydroxy-10,11-dehydrocurvularin (4): Colourless amorphous solid (4.3 mg, 0.1%), $[\alpha]_{\text{D}}^{25} = +126.5$ ($c = 0.29$, EtOH). UV (EtOH): λ_{max} (ϵ) = 224 (12710), 298 (7351), 336 nm (5972). CD ($c = 1.6 \times 10^{-3}$ mol/L, MeOH): λ_{max} ($\Delta\epsilon$) = 231 (+5.49), 297 (+1.07), 335 nm (−0.27). IR (ATR): $\tilde{\nu}_{\text{max}}$ = 3315 (br), 2926, 1707, 1620, 1591, 1252 and 1181 cm^{-1} . ^1H and ^{13}C NMR spectroscopic data (Tables S1 and S2, Supporting Information); LRESIMS: m/z = 307 $[\text{M} + \text{H}]^+$. HRESIMS calcd. for C₁₆H₁₉O₆ $[\text{M} + \text{H}]^+$ m/z 307.1182, found m/z 307.1179.

(+)-(11S,15R)-11-Hydroxycurvularin (5): Colourless amorphous solid (7.0 mg, 0.2%), $[\alpha]_{\text{D}}^{22} = +6.9$ ($c = 0.47$, EtOH). UV (EtOH): λ_{max} (ϵ) = 223 (9383), 274 (5270), 306 nm (4370). CD ($c = 1.6 \times 10^{-3}$ mol/L, MeOH): λ_{max} ($\Delta\epsilon$) = 229 (+5.06), 271 (−2.21), 326 nm (+2.11). IR (ATR): $\tilde{\nu}_{\text{max}}$ = 3294 (br), 2928, 1698, 1610, 1592, 1268 and 1161 cm^{-1} . ^1H and ^{13}C NMR spectroscopic data (Tables S1 and S2, Supporting Information); LRESIMS: m/z = 309 $[\text{M} + \text{H}]^+$. HRESIMS calcd. for C₁₆H₂₁O₆ $[\text{M} + \text{H}]^+$ m/z 309.1338, found m/z 309.1333.

(+)-(11R,15R)-11-Hydroxycurvularin (6): Colourless amorphous solid (3.9 mg, 0.1%), $[\alpha]_{\text{D}}^{22} = +25.2$ ($c = 0.26$, EtOH). UV (EtOH): λ_{max} (ϵ) = 222 (11265), 274 (6790), 306 nm (5556). CD ($c = 1.6 \times 10^{-3}$ mol/L, MeOH): λ_{max} ($\Delta\epsilon$) = 229 (+1.20), 239 (−0.89), 272 (−0.50), 327 nm (+3.12). IR (ATR): $\tilde{\nu}_{\text{max}}$ = 3272 (br), 2930, 1698, 1610, 1591, 1271 and 1167 cm^{-1} . ^1H and ^{13}C NMR spectroscopic data (Tables S1 and S2, Supporting Information); LRESIMS: m/z = 309 $[\text{M} + \text{H}]^+$. HRESIMS calcd. for C₁₆H₂₁O₆ $[\text{M} + \text{H}]^+$ m/z 309.1338, found m/z 309.1333.

(+)-(15R)-12-Oxocurvularin (7): Colourless amorphous solid (1.2 mg, 0.03%), $[\alpha]_{\text{D}}^{22} = +53.8$ ($c = 0.13$, EtOH). UV (EtOH): λ_{max} (ϵ) = 221 (11237), 272 (5335), 300 nm (4200). CD ($c = 1.6 \times 10^{-3}$ mol/L, MeOH): λ_{max} ($\Delta\epsilon$) = 230 (+3.73), 266 (−1.58), 320 nm (+1.86). IR (ATR): $\tilde{\nu}_{\text{max}}$ = 3348 (br), 2928, 1704, 1609, 1592, 1272 and 1162 cm^{-1} . ^1H and ^{13}C NMR spectroscopic data (Tables S1 and S2, Supporting Information); LRESIMS: m/z = 307 $[\text{M} + \text{H}]^+$. HRESIMS calcd. for C₁₆H₁₆O₅ $[\text{M} - \text{H}_2\text{O}]^+$ m/z 288.0998, found m/z 288.1001.

Compound 8: Yellowish amorphous solid (13.9 mg, 0.4%), $[\alpha]_{\text{D}}^{23} = -9.1$ ($c = 0.4$, EtOH). UV (MeOH): λ_{max} (ϵ) = 221 (19520), 273 (8046), 305 nm (6867). CD ($c = 9.5 \times 10^{-4}$ mol/L, MeOH): λ_{max} ($\Delta\epsilon$) = 222 (−2.08), 236 (+3.09), 264 (−1.06), 285 (+0.73), 305 (−1.77), 327 nm (+3.49). IR (ATR): $\tilde{\nu}_{\text{max}}$ = 3285 (br), 2933, 1702, 1612, 1591, 1272 and 1163 cm^{-1} . ^1H and ^{13}C NMR spectroscopic data (Table 3); LRESIMS: m/z = 581 $[\text{M} + \text{H}]^+$. HRESIMS calcd. for C₃₂H₃₆O₁₀ $[\text{M}]^+$ m/z 580.2309, found m/z 580.2309.

Cytotoxicity Testing: A modified propidium iodide monolayer assay was used to determine the cytotoxic activity of the compounds against human tumor cell lines. The test procedure has been described elsewhere.^[31] Cell lines tested were derived from patient tumors engrafted as a subcutaneously growing tumor in NMRI nu/nu mice, or obtained from the American Type Culture Collection, Rockville, MD, National Cancer Institute, Bethesda, MD, or Deutsche Sammlung von Mikroorganismen und Zellkulturen, Braunschweig, Germany. Briefly, human tumor cells lines were grown at 37 °C in a humidified atmosphere (95% air, 5% CO₂) in monolayer cultures in RPMI 1640 medium supplemented with 10% FCS and phenol red (PAA, Cölbe, Germany). Cells were trypsinized and maintained weekly. Cells were harvested from exponentially growing cultures by trypsinization, counted and plated in 96 well flat-bottomed micro plates (140 μL cell suspension, 5×10^3 to 10×10^3 cells/well). After a 24 h recovery to allow cells to resume exponential growth, 10 μL of culture medium (6 control wells per plate) or medium containing the test drug were added to the wells. Each drug concentration was plated in triplicate. After 4 days of incubation the culture medium was replaced by fresh medium containing 6 $\mu\text{g/mL}$ of propidium iodide. Microplates were then kept at −18 °C for 24 h, to give a total cell kill. After thawing of the plates, fluorescence was measured using the Cytofluor 4000 microplate reader (Perseptive Biosystems) (excitation 530 nm, emission 620 nm). The amount of viable cells was proportional to the fluorescence intensity. Cytotoxicity including the induction of apoptosis and the inhibition of cell proliferation was recorded as a reduction of the viable cell number relative to control wells and expressed as T/C (test/control) value.

Data Evaluation, Mean Graph Analysis: Antiproliferative efficacies of test compounds were described by inhibitory concentrations (IC₅₀ values), reflecting concentration-dependent cytotoxicity. Extrapolated IC₅₀ values were given if the exact value could not be determined within the test range, and if linear regression of existing T/C values resulted in IC₅₀ values within a range of threefold the highest test concentration. In the case of resistant cell lines, exhibit-

ing no activities, IC_{50} values were expressed to be greater than the highest test concentration. Cytotoxic selectivity patterns were obtained by mean graph analyses, where the distribution of IC_{50} values obtained for a test compound in the individual tumor types was given in relation to the mean IC_{50} value, obtained for all tumors tested. The individual IC_{50} values were expressed as bars on a logarithmically scaled axis. Bars to the left demonstrated IC_{50} values lower than the mean value (indicating more sensitive tumor models), bars to the right demonstrated higher values (indicating rather resistant tumor models).

Supporting Information (see also the footnote on the first page of this article): NMR and CD spectra of **1–8**, NMR spectroscopic data of **2–7**, and detailed cytotoxicity data of **1, 2, 4, 5**, and **6**.

Acknowledgments

We thank Carsten Siering and Prof. Dr. Siegfried Waldvogel, Kekulé-Institute for Organic Chemistry and Biochemistry, University of Bonn, Germany, for giving us the opportunity to use the CD spectropolarimeter. Special thanks to Ciemon Frank V. Caballes and Pablo Jong T. Rojas Jr., for generous assistance and support at the Marine Laboratory, University of Guam, USA. P. J. S. acknowledges funding by the National Institutes of Health (NIH), MBRS SCORE, S06-GM44796. This work is contribution number 619 of the University of Guam Marine Laboratory. Financial support from the German Bundesministerium für Bildung und Forschung (BMBF) (Project No. 03F0415A) is gratefully acknowledged.

- [1] a) W. H. Urry, H. L. Wehrmeister, E. B. Hodge, P. H. Hidy, *Tetrahedron Lett.* **1966**, 7, 3109–3114; b) R. N. Mirrington, E. Ritchie, C. W. Shoppee, W. C. Taylor, *Tetrahedron Lett.* **1964**, 5, 365–370; c) N. Winssinger, S. Barluenga, *Chem. Commun.* **2007**, 22–36; d) A. J. Birch, O. C. Musgrave, R. W. Rickards, H. Smith, *J. Chem. Soc.* **1959**, 3146–3152.
- [2] R. J. Miksicek, *J. Steroid Biochem. Mol. Biol.* **1994**, 49, 153–160.
- [3] S. V. Sharma, T. Agatsuma, H. Nakano, *Oncogene* **1998**, 16, 2639–2645.
- [4] T. Agatsuma, Y. Kanda, H. Onodera, M. Hideyuki, N. Matsushita, T. Ogawa, S. Akinaga, S. Soga, WO 2004024141 A1 20040325, **2004**.
- [5] Y. L. Janin, *J. Med. Chem.* **2005**, 48, 7503–7512.
- [6] I. Gaffoor, F. Trail, *Appl. Environ. Microbiol.* **2006**, 72, 1793–1799.
- [7] a) K. Arai, B. J. Rawlings, Y. Yoshizawa, J. C. Vederas, *J. Am. Chem. Soc.* **1989**, 111, 3391–3399; b) Y. Liu, Z. Li, J. C. Vederas, *Tetrahedron* **1998**, 54, 15937–15958.
- [8] a) H. Greve, S. Meis, M. U. Kassack, S. Kehraus, A. Krick, A. D. Wright, G. M. König, *J. Med. Chem.* **2007**, 50, 5600–5607; b) H. Greve, S. Kehraus, A. Krick, G. Kelter, A. Maier, H.-H. Fiebig, A. D. Wright, G. M. König, *J. Nat. Prod.* **2008**, 71, 309–312.
- [9] K. Hanasaki, T. Kamigaito, JP 2000287697 A 20001017 (Japanese patent), **2000**.
- [10] a) H. Fu, S. Ebert-Koshla, D. A. Hopwood, C. Koshla, *J. Am. Chem. Soc.* **1994**, 116, 4166–4170; b) H. Fu, D. A. Hopwood, C. Koshla, *Chem. Biol.* **1994**, 1, 205–210.
- [11] a) H. D. Munro, O. C. Musgrave, R. Templeton, *J. Chem. Soc. C* **1967**, 947–948; b) J. Zhan, E. M. K. Wijeratne, C. J. Seliga, J. Zhang, E. E. Pierson, L. S. Pierson III, H. D. Vanetten, A. A. L. Gunatilaka, *J. Antibiot.* **2004**, 57, 341–344.
- [12] S. Lai, Y. Shizuri, S. Yamamura, K. Kawai, H. Furukawa, *Bull. Chem. Soc. Jpn.* **1991**, 64, 1048–1050.
- [13] S. Lai, Y. Shizuri, S. Yamamura, K. Kawai, Y. Terada, H. Furukawa, *Tetrahedron Lett.* **1989**, 30, 2241–2244.
- [14] H. Gerlach, *Helv. Chim. Acta* **1977**, 60, 3039–3044.
- [15] B. Bicalho, R. A. C. Goncalves, A. P. M. Zibordi, G. P. Manfio, A. J. Marsaioli, *Z. Naturforsch., Teil C, J. Biosci.* **2003**, 58, 746–751.
- [16] a) R. A. Edrada, M. Heubes, G. Brauers, V. Wray, A. Berg, U. Gräfe, M. Wohlfarth, J. Mühlbacher, K. Schaumann, Sudarsono, G. Bringmann, P. Proksch, *J. Nat. Prod.* **2002**, 65, 1598–1604; b) Y. Murakami, A. Ishii, S. Mizuno, S. Yaginuma, Y. Uehara, *Anticancer Res.* **1999**, 19, 4145–4150.
- [17] a) D. C. Aldridge, S. Galt, D. Giles, W. B. Turner, *J. Chem. Soc. C* **1971**, 1623–1627; b) H. Oyama, T. Sassa, M. Ikeda, *Agric. Biol. Chem.* **1978**, 42, 2407–2409; c) C. J. Barrow, *J. Nat. Prod.* **1997**, 60, 1023–1025; d) E. A. Couladouros, A. P. Mihou, E. A. Bouzas, *Org. Lett.* **2004**, 6, 977–980.
- [18] S. Lai, Y. Shizuri, S. Yamamura, K. Kawai, Y. Terada, H. Furukawa, *Chem. Lett.* **1990**, 589–592.
- [19] a) S. B. Hyeon, A. Ozaki, A. Suzuki, S. Tamura, *Agric. Biol. Chem.* **1976**, 40, 1663–1664; b) D. J. Robeson, G. A. Strobel, R. N. Strange, *J. Nat. Prod.* **1985**, 48, 139–141.
- [20] a) M. Kusano, K. Nakagami, S. Fujioka, T. Kawano, A. Shimada, Y. Kimura, *Biosci. Biotechnol. Biochem.* **2003**, 67, 1413–1416; b) J. He, E. M. K. Wijeratne, B. P. Bashyal, J. Zhan, C. J. Seliga, M. X. Liu, E. E. Pierson, L. S. Pierson III, H. D. VanEtten, A. A. L. Gunatilaka, *J. Nat. Prod.* **2004**, 67, 1985–1991.
- [21] J. F. Grove, *J. Chem. Soc. C* **1971**, 2261–2263.
- [22] P. M. Dewick, *Medicinal Natural Products: A Biosynthetic Approach*, 2nd ed., John Wiley & Sons, Chichester, England, **2001**, pp. 149–150.
- [23] a) Y. Zhang, X. M. Li, B. W. Wang, *J. Antibiot.* **2007**, 60, 204–210; b) H. A. Priestap, *Tetrahedron* **1984**, 40, 3617–3624; c) J. L. Bloomer, T. J. Caggiano, C. A. Smith, *Tetrahedron Lett.* **1982**, 23, 5103–5106.
- [24] a) M. Isaka, S. Palasarn, K. Kocharin, J. Saenboonrueng, *J. Nat. Prod.* **2005**, 68, 945–946; b) A. Krick, S. Kehraus, C. Gerhäuser, K. Klimo, M. Nieger, A. Maier, H. H. Fiebig, I. Atodiresei, G. Raabe, J. Fleischhauer, G. M. König, *J. Nat. Prod.* **2007**, 70, 353–360.
- [25] a) T. S. Bugni, V. S. Bernan, M. Greenstein, J. E. Janso, W. M. Maiese, C. L. Mayne, C. M. Ireland, *J. Org. Chem.* **2003**, 68, 2014–2017; b) V. Rukachaisirikul, S. Chantaruk, W. Pongcharoen, M. Isaka, S. Lapanun, *J. Nat. Prod.* **2006**, 69, 980–982; c) A. Evidente, G. Randazzo, N. S. Iacobellis, A. Bottalico, *J. Nat. Prod.* **1985**, 48, 916–923; d) A. K. Demetriadou, E. D. Laue, F. J. Leeper, J. Staunton, *J. Chem. Soc., Chem. Commun.* **1985**, 762–764.
- [26] P. M. Dewick, *Medicinal Natural Products: A Biosynthetic Approach*, 2nd ed., John Wiley & Sons, Chichester, England, **2001**, pp. 101–103.
- [27] a) G. R. Pettit, J. P. Xu, D. L. Doubek, J. C. Chapuis, J. M. Schmidt, *J. Nat. Prod.* **2004**, 67, 1252–1255; b) G. R. Pettit, C. L. Herald, D. L. Doubek, D. L. Herald, *J. Am. Chem. Soc.* **1982**, 104, 6846–6848.
- [28] a) S. A. Hitchcock, G. Pattenden, *Tetrahedron Lett.* **1990**, 31, 3641–3644; b) H. G. Cutler, R. F. Arrendale, J. P. Springer, P. D. Cole, R. G. Roberts, R. T. Hanlin, *Agric. Biol. Chem.* **1987**, 51, 3331–3338; c) M. Lampilas, R. Lett, *Tetrahedron Lett.* **1992**, 33, 777–780.
- [29] T. Yoshino, F. Ng, S. J. Danishefsky, *J. Am. Chem. Soc.* **2006**, 128, 14185–14191.
- [30] G. Bringmann, P. Proksch, R. A. Edrada, M. Heubes, E. Gunther, US 2003216354 A1 20031120, **2003**.
- [31] W. A. Dengler, J. Schulte, D. P. Berger, R. Mertelsmann, H. H. Fiebig, *Anticancer Drugs* **1995**, 6, 522–532.

Received: May 29, 2008

Published Online: September 11, 2008